Search for methane and upper limits to ethane and SO$_2$ on Mars

Vladimir A. Krasnopolsky [1]

Department of Physics, Catholic University of America, Washington, DC 20064, United States

ABSTRACT

The IRTF/CSHELL observations in February 2006 at L_S = 10° and 63–93°W show ~10 ppb of methane at 45°S to 7°N and ~3 ppb outside this region that covers the deepest canyon Valles Marineris. Observations in December 2009 at L_S = 20° and 0–30°W included spectra of the Moon at a similar airmass as a telluric calibrator. A technique for extraction of the martian methane line from a combination of the Mars and Moon spectra has been developed. The observations reveal no methane with an upper limit of 8 ppb. The results of both sessions agree with the observations by Mumma et al. (Mumma, M.J. et al. [2009]. Science 323, 1041–1045) at the same season in February 2006 and are smaller than those in the PFS and TES maps. Production and removal of the biological methane on Mars do not significantly change the redox state of the atmosphere and the balance of hydrogen. A search for ethane at 2977 cm^{-1} results in an upper limit of 0.2 ppb. However, this limit does not help to establish the origin of methane on Mars. Reanalysis of our search for SO$_2$ using TEXES confirms the recently established upper limit of 0.3 ppb. Along with the lack of hot spots and gas vents with endogenic heat sources in the THEMIS observations, the very low upper limit to SO$_2$ on Mars does not favor geological methane that is less abundant than SO$_2$ in the outgassing from the terrestrial planets.

© 2011 Elsevier Inc. All rights reserved.

1. Introduction

Currently a few teams have published their observations of methane on Mars. Krasnopolsky et al. (2004a,b) searched for the P-branch of the CH$_4$ band at 3.3 μm on Mars using the Fourier Transform Spectrometer at the Canada–France–Hawaii Telescope with resolving power of 180,000. Their observation was made in January 1999 at L_S = 88° and found a mean CH$_4$ abundance of 10 ± 3 ppb, near the 3-sigma detection limit.

The Planetary Fourier Spectrometer (PFS) at the Mars Express orbiter (MEX) has an effective (two sampling points) resolving power of 1500, and the Q-branch at 3018 cm^{-1} is the best spectral feature to search for methane with this instrument (Formisano et al., 2004). Although this feature is below the noise level in the individual spectra, regular observations for six years resulted in 500,000 spectra that were grouped and averaged to study variations of methane on Mars. The latest PFS paper (Geminale et al., 2011) presents a zonally averaged seasonal–latitudinal map of methane and maps for four seasons that cover a latitude range of 120° with a grid of 20° × 20°. The CH$_4$ mixing ratio varies from 0 to 70 ppb with a global-mean value of 15 ppb. One should bear in mind that averaging of a few thousand spectra, which was made

to get measurable methane absorption, may not remove instrumental effects and other sources of systematic error.

Mumma et al. (2009) searched for methane on Mars at three observatories. They reported variations of methane with latitude and season from 30 to 300 ppb at a few conference talks before 2007. However, they show in their published paper only the results of three observing sessions with IRTF/CSHELL in January 2003, March 2003, and February 2006, and the observed methane varies from 0 to 40 ppb. Therefore the results of Mumma et al. (2009) remove the previously existing inconsistency between their mean CH$_4$ abundances and those measured by the other teams.

Fonti and Marzo (2010) analyzed the MGS/TES spectra that cover the CH$_4$ band at 1306 cm^{-1}. The TES spectral resolving power is low, ~100 and ~200, its noise is 1.2×10^{-8} W cm^{-1} sr^{-1}, and averaging of 11,000 and 3000 spectra is required to achieve a detection limit of 10 ppb, respectively (Fonti and Marzo, 2010). They chose 3×10^6 dayside spectra in the latitude range of ±60° and then selected to a methane cluster of 9.3×10^5 spectra that favored the detection of methane. Eleven seasonal maps of methane that cover three martian years are the final products of this study.

Although the maps show numerous details, one should bear in mind that those eleven maps represent 103 detection points using the above values. ($9.3 \times 10^5/11,000 \approx 85$; correction for regions observed with the resolving power of 200 results 103 points.) Therefore the mean number of the effective points is ~9 per map, and four maps are based on ~4 points per map. Their approach is not standard, and it is not clear that the clustering does not break the true statistics of the signal near 1306 cm^{-1}.

Various aspects of the problem of methane on Mars are considered in the cited papers and in Krasnopolsky (2006), Lefevre and Forget (2009), and Mischna et al. (2011). The latter two papers present simulations of the methane behavior on Mars using Mars general circulation models. A brief review of the problem may be found in Krasnopolsky (2011). Recently Zahnle et al. (2011) question the detections of methane by all four teams. They also argued that the observational data on variable methane are inconsistent with the redox state of the martian atmosphere.

Here we will consider our observations of methane on Mars in 2006 and 2009. The observations in 2009 utilized a technique of comparison of spectra of Mars and the Moon. Then we will describe our attempt to detect ethane and revise our upper limit to SO_2 on Mars.

2. Observing instruments and conditions

Mumma et al. (2009) concluded that the CSHELL spectrograph at the NASA Infrared Telescope Facility is currently among the best instruments for ground-based observations of methane on Mars. We are using this instrument for more than a decade to study chemical compositions of the atmospheres of Mars and Venus and their variations (see, for example, Krasnopolsky (2007, 2010b)).

CSHELL is a long-slit echelle spectrograph for a spectral range of 1.08–5.6 μm. Its slit is 30×0.5 arcsec^2 in our observations, a chosen spectral interval is $0.0023\nu_0$ (ν_0 is the central wavenumber), and the detector is an InSb array of 256×150 pixels cooled to 30 K. Main parts of the instrument are also cooled by liquid nitrogen. The pixel size is 0.2×0.2 arcsec^2 and $9 \times 10^{-6}\nu_0$ in the dispersion direction. The instrument resolving power is $\nu/\delta\nu = 40{,}000$. The telescope diameter is 3 m; its position on Mauna Kea (Hawaii) with elevation of 4.2 km, atmospheric pressure of 0.6 bar, and mean overhead water of 2 mm is favorable for spectroscopy of the planetary atmospheres.

Observations of martian spectral lines against similar telluric lines are possible due to the Doppler shift from Mars geocentric velocity when the Earth is approaching and then leaving Mars. The best conditions for the observations are typically two months before and after the opposition, when the geocentric velocity may be as high as 17 km s^{-1} while the Mars size is ~10 arcsec.

The R0 and R1 lines at 3028.752 cm^{-1} and 3038.498 cm^{-1} with line strengths of 1.65×10^{-19} cm and 1.55×10^{-19} cm at 200 K, respectively, are the best for ground-based detection of methane on Mars. Mumma et al. (2009, Supporting material) calculated the uncertainty caused by photon statistics at 0.12% of the signal; a similar value should be added to account for the flat field uncertainty. These values are calculated for the unattenuated spectrum of Mars, while the CH_4 lines are observed at the wings of the very strong telluric lines, where the transmission is 0.3–0.4 (Fig. 1) and the above values should be doubled. Then a total inevitable uncertainty is $2(2 \times 0.12^2)^{1/2} = 0.34\%$. Being referred to an interval of 0.1 cm^{-1} (3.7 pixels) that acquires 90% of the line absorption, it results in an uncertainty of the retrieved methane mixing ratio

$$\delta f_{CH4} = \frac{0.0034 \times 0.1}{2.5 \times 3.7^{1/2} \times S \times N_0} = 2 \text{ ppb}.$$

Here 2.5 is the two-way airmass, S is the line strength, and $N_0 = 2.3 \times 10^{23}$ cm^{-2} is the molecular column abundance in the 6.1 mbar atmosphere of Mars. The signal varies by a factor of ~3 within the interval of 3.7 pixels centered at the position of the martian line (Fig. 1), and it is very difficult to detect a deviation of ~0.5% at this steep slope.

There are ~200 bad or unstable pixels in the detector array of 38,400 pixels. Some pixels in the observed spectral frames are af-
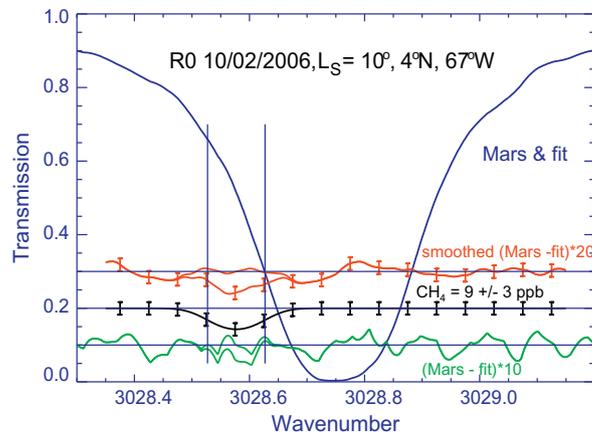

Fig. 1. The best spectral fit to the observed CH_4 R0 line. The observed and synthetic spectra are not distinguishable, and their difference is shown at the bottom scaled by a factor of 10 with and without the martian methane (green curves). Interval of 0.1 cm^{-1} centered at the expected position of the martian methane is marked by the vertical lines. The green curves smoothed within 0.1 cm^{-1} are shown red with their corrected standard deviation. The black curve is difference between the red curves and depicts the martian methane which abundance is equal to 9 ± 3 ppb. (For interpretation of the references to color in this figure legend, the reader is referred to the web version of this article.)

fected by charged particle events from the cosmic rays and natural radioactivity. Their readings are replaced by the means of their two neighbors and add to the uncertainty. However, these icky pixels are seen if they differ from the neighbors by more than ~3% in regular parts of the spectra and ~15% near the positions of the martian methane lines on the steep wings of the telluric CH_4 lines. The smaller deviations from these weakly unstable pixels are another source of uncertainty. Their behavior and statistics are poorly predictable.

Observing conditions for two sessions of our observations of methane in 2006, 2009, and ethane in 2007 are given in Table 1. Our observations of methane are typically made using 8-min exposures with the slit position along the central meridian. The telescope pointing may change for a longer exposure time, and a pointing correction is made using the CSHELL direct imaging mode. Then the instrument is switched back to the spectroscopic mode; however, the slit position relative to the instrument parts is not exactly the same, the next spectra cannot be simply coadded and are processed separately. The spectral frames are corrected for dark current, flat field from a continuum source, and bad and unstable pixels.

Each frame is a set of 150 spectra of 256 pixels with ~50 spectra of Mars and the remaining ~100 spectra of the foreground. To improve the accuracy, each spectrum is transformed into 2048 sampling points using a parabolic interpolation by a method described in Krasnopolsky (2007). Then a wavenumber scale is determined for each spectrum using positions of the foreground

Table 1
Observing conditions.

	10/02/2006	18/10/2007	07/12/2009
Date	10/02/2006	18/10/2007	07/12/2009
L_S	10°	331°	20°
Diameter (arcsec)	8.1	11.0	10.4
Heliocentric velocity (km s^{-1})	2.0	2.2	1.8
Geocentric velocity (km s^{-1})	17.3	−11.3	−13.0
Subearth latitude	−13.5°	6°	19°
Mean east longitude of CM	282°	73°	345°
Mean local time	9.7	14.4	14.2
Phase angle	38°	40°	33°

CM is central meridian, phase angle is the Sun–planet–Earth angle.

emission lines. Next the spectra are linearly interpolated to a uniform wavenumber scale with a step of 0.001 cm^{-1}. Then the martian spectra are corrected for the foreground (see below). Finally, three consecutive spectra are summed up to improve the uncertainty and give ~15 spectra with effective exposure time of 24 min for further analysis.

3. Observations in February 2006

Our previous analysis of the IRTF/CSHELL observations of methane on Mars in February 2006 gave an upper limit of 14 ppb after averaging of all data from the two lines (Krasnopolsky, 2007). The achieved uncertainty was mainly caused by uncertainties of fitting the observed spectra by synthetic spectra. The observations were made at perfect conditions of the best geocentric velocity (17.3 km s^{-1}), low overhead water (0.5 pr. mm), Mars near the zenith, and excellent seeing.

Here we will try to improve the spectral fitting to the observations in February 2006. We choose for fitting 33 pixels centered at the CH$_4$ R0 line at 3028.752 cm^{-1} in each spectrum. Seven fitting parameters refer to the observed spectrum: the instrument sensitivity as a parabolic function of wavenumber, scattered light in the spectrum, spectral resolution described by a Gaussian, and two wavenumber corrections. The ACE solar spectrum (Hase et al., 2010) is properly shifted for both geocentric and heliocentric velocities. The H$_2$O telluric lines are weak in the chosen spectrum and calculated using a fixed overhead water of 0.48 pr. mm (Krasnopolsky, 2007). The CH$_4$ telluric lines are calculated using the CH$_4$ column abundance, its mean pressure and temperature. The line optical depth at wavenumber v integrated from the bottom to the infinity is

$$\tau_v = \frac{\mu S N}{4\pi\delta v} ln\left[1 + \left(\frac{2\delta v}{v - v_0}\right)^2\right]$$

(Krasnopolsky et al., 1997). Here μ is the airmass, N is the column abundance, S is the line strength, and δv is the collisional line half-width at the mean pressure and temperature. This relationship was derived for an isothermal atmosphere and a constant mixing ratio of an absorber.

The O$_3$ telluric absorption is given by the O$_3$ column abundance and mean temperature. The O$_3$ line depths in the line center are smaller than one; however, we apply a curve of growth that was calculated using the Voigt line shape and the mean pressure of 25 mbar typical of the ozone maximum near 25 km.

If the martian lines are shifted to the blue, then the ^{13}CH$_4$ isotope lines overlap the martian methane line with a significant error in its extraction. That was mentioned by Krasnopolsky (2007) and considered in detail by Zahnle et al. (2011) who doubt in the results of Mumma et al. (2009) observed at the blue shift in 2003. Our observations in February 2006 are at the red shift, and we correct the ^{13}CH$_4$ line strengths from the HITRAN spectroscopic database by a factor of 0.953 (Zahnle et al., 2011) that reflects the smaller content of this isotope in the Earth's atmosphere relative to the PDB standard adopted in the HITRAN.

Least square fitting to a spectrum at 4°N and 67°W is exposed in Fig. 1. This fitting is identical to the χ^2-fitting for a constant uncertainty. The difference between the observed and synthetic spectra is shown with and without the martian methane line. This difference smoothed within 0.1 cm^{-1} gives the martian line equivalent width. Its uncertainty is equal to the standard deviation of the smoothed curve times $[(33 - 1)/(33 - 13)]^{1/2} = 1.27$. Here 33 is the number of degrees of freedom (pixels) and 13 is the number of fitting parameters.

Pressure and temperature at a half pressure level at each observing point in the martian atmosphere are taken from the MGS/TES observations (Conrath et al., 2000; Smith, 2004). TES ceased in January 2006, and we use the TES data in March 2004 for the similar L_S, latitudes and longitudes. These pressures and temperatures are applied to convert the retrieved CH$_4$ line equivalent widths into the methane mixing ratios.

The CH$_4$ mixing ratios derived in three observations of the R0 line along the central meridian on February 10 2006 are shown in Fig. 2. The retrieved abundances at 4°N are similar in all three observations; that is why we have chosen one of those in Fig. 1. The methane uncertainty in the spectrum in Fig. 1 is 3 ppb, above 2 ppb calculated in the previous section. However, a typical uncertainty is ~5 ppb because of the imperfect correction of the bad pixels. The scatter of the points from the mean latitudinal dependence in Fig. 2 varies from 1 to 10 ppb with a mean value of 5 ppb as well. Both the uncertainties of the retrieved mixing ratios and their place-to-place variations contribute to the scatter.

The mean curve in Fig. 2 indicates three regions with different methane abundances. Averaging of the data gives 1.7 ± 1.2 ppb at 80–45°S, 10 ± 2 ppb at 45°S to 7°N, and 4.4 ± 1.2 ppb at 7–55°N. The given uncertainties do not include possible systematic errors that are not ruled out in such a fine procedure as the extraction of the martian methane from the IRTF/CSHELL spectra.

The MOLA map of the region with the greater methane abundance is shown in Fig. 3. It covers the deepest canyon Valles Marineris. Maybe specific conditions of the deep canyon facilitate biological or geological production of methane.

Our results are in reasonable agreement with the observation by Mumma et al. (2009) on February 26 2006, just two weeks after our observation. They measured ~3 ppb from 60°S to 20°N and less than 2 ppb at 20–50°N. Longitude was 137°E in their observation.

The PFS zonally-averaged seasonal–latitudinal map (Geminale et al., 2011, their fig. 4) gives ~25 ppb at $L_S = 10°$ and latitudes ±50°. Their map for northern spring shows at 60–100°W the CH$_4$ mixing ratio varying from 20 to 50 ppb between 50°S and 50°N. (Here and below we approximately convert colors on the maps into the methane column abundances and then to its mixing ratios.)

The TES maps at latitudes ±60° (Fonti and Marzo, 2010) for northern spring give at 60–90°W ~25 ppb in 2000, ~20 ppb in 2002, and ~15 ppb in 2004. The methane abundances in these maps are typically larger at latitudes of 40–60° than those at the low latitudes. This behavior is opposite to that observed by Mumma et al. (2009) and in our Fig. 2.

The observed spectra of the CH$_4$ R1 line are not so good for the extraction of martian methane because the position of the martian Doppler-shifted methane line at 3038.325 cm^{-1} coincides with the O$_3$ line at 3038.323 cm^{-1}. The O$_3$ line equivalent width is equal to that of the CH$_4$ line for a mixing ratio of ~35 ppb on Mars. Though the O$_3$ line is constrained by other O$_3$ lines in the spectrum, this coincidence lowers the accuracy of the methane extraction. Furthermore, only two lines in the R1 spectra may be used for the wavenumber calibration. This situation could be improved by
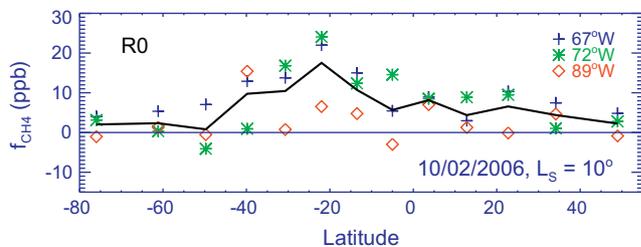

Fig. 2. Retrieved methane mixing ratios along the central meridian in three observations of the CH$_4$ R0 line in February 2006. Mean results for all latitudes are shown by the solid line.
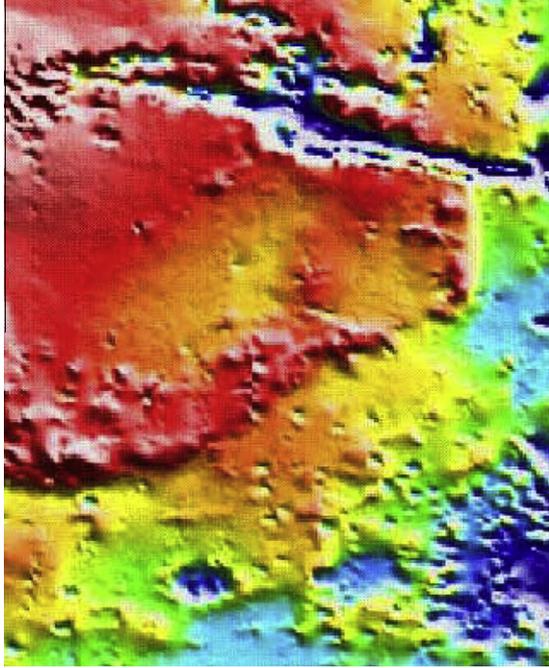
Fig. 3. Fragment of the MOLA map of Mars at 260–310°E, 60°S to 0° that includes a region at 265–300°E and 45°S to 7°N with ~10 ppb of methane in February 2006.
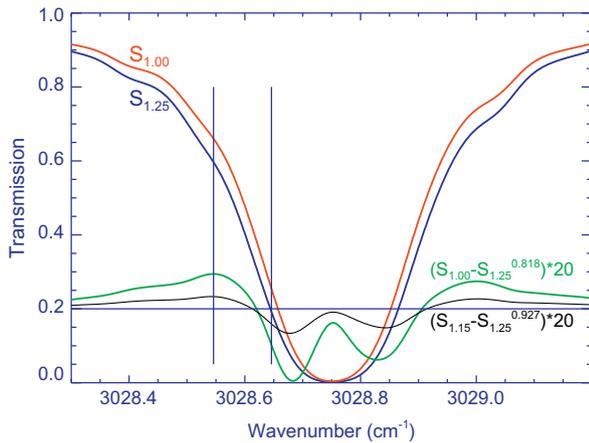

Fig. 4. Numerical simulation for comparison of spectra of Mars ($S_{1.00}$, red) and the Moon ($S_{1.25}$, blue) observed at airmasses of 1.00 and 1.25, respectively. Their difference for fitting by the power function is scaled by a factor of 20 (green). The black line shows a similar difference for Mars observed at airmass of 1.15. Vertical lines show interval of 0.1 cm^{-1} at the martian R0 line for geocentric velocity of 15 km s^{-1}. (For interpretation of the references to color in this figure legend, the reader is referred to the web version of this article.)

measuring spectra of the CSHELL Ar and Xe lamps during the observations; however, that has not been made.

4. Using the Moon spectra to compensate for telluric absorption

Later we came to conclusion that extraction of methane absorption from the IRTF/CSHELL spectra of Mars may be improved by comparison with spectra of the Moon observed simultaneously and by the same instrument. Some instrumental errors may cancel out or reduce in this comparison. Fitting by synthetic spectra is not required in this case. We observed both Mars and the Moon at the CH$_4$ R0 and R1 lines on December 7, 2009.

Absorption in the Earth's atmosphere of light I_i from an external source is accompanied by thermal emission:

$$dI_i = -I_i(\tau_i)d\tau_i + B(\tau_i)d\tau_i.$$

Here τ_i is the slant optical depth in the Earth's atmosphere and $B(\tau_i)$ is the blackbody thermal emission at temperature $T(\tau_i)$. Integration of this differential equation results in

$$I_i(\tau_i) = I_{0i}e^{-\tau_i} + e^{-\tau_i}\int_0^{\tau_i} B(t)e^t dt = I_{0i}e^{-\tau_i} + f_i.$$

The second term is the foreground emission, and subtraction of the foreground spectrum measured near the target from the target spectrum corrects the latter for the thermal emission in the Earth's atmosphere. We have found that subtraction of the interpolated foreground from the same frame is more accurate that using the foreground frames measured off the basic frame.

Both thermal emission and reflected sunlight contribute to the spectrum of the target:

$$I_{0i} = a(1 + a_0S_i); \quad sp_i = a(1 + a_0S_i)e^{-\tau_i} = I_i - f_i.$$

Here S_i is the Doppler-shifted solar spectrum near the methane R0 or R1 line. Absorption lines are weak in that spectrum, and $S_i \approx 1$. Parameters a and a_0 describe intensities of the thermal emission and sunlight, reflectivity of the target, and the instrument sensitivity. A similar relationship for a spectrum of the Moon I_{mi} is

$$b(1 + b_0S_{0i})e^{-\frac{\tau_i}{c}} = I_{mi} - c_0f_i.$$

Here b and b_0 are the analogs to a and a_0, S_{0i} is the unshifted solar spectrum, and c reflects difference between airmasses of the target and the Moon.

The whole frame is covered by the Moon, and the foreground spectrum is taken from the target frame with a correction factor c_0. The last relationship may be transformed to

$$e^{-\tau_i} = \frac{(I_{mi} - c_0f_i)^c}{b^c(1 + b_0S_{0i})^c} = \frac{(I_{mi} - c_0f_i)^c}{b^c(1 + cb_0S_{0i} + \cdots)}.$$

Thermal emission of bright parts of the Moon is much stronger than the reflected sunlight at 3.3 μm, and the higher terms in the denominator may be neglected. Then the relationship for the Moon spectrum to fit the Mars spectrum is

$$m_i = a(1 + a_0S_i)e^{-\tau_i} = a\frac{(I_{mi} - c_0f_i)^c(1 + a_0S_i)}{b^c(1 + cb_0S_{0i})}.$$

It may be written as

$$m_i = \frac{b_0(I_{mi} - b_3f_i)^{b_4}}{1 + b_1i + b_2i^2} \times \frac{S_i + b_5}{S_{0i} + b_6}.$$

Here the denominator reflects a weak but not negligible variation of the instrument sensitivity within a chosen spectral interval. Thus, using the observed spectra of the target I_i, the foreground f_i, and the Moon I_{mi} and the known solar spectrum S_i, it is possible to fit sp_i by m_i by varying the parameters b_{0-6}. One more parameter is the wavenumber shift between the target and Moon spectra, which is of the order of 0.001 cm^{-1}.

The least square fitting is made by minimizing the difference $\sum_i(sp_i - m_i)^2$. A small interval of 0.1 cm^{-1} (1.35 times the resolution element) centered at the expected Doppler-shifted position of the martian methane line is not involved in the fitting. Then a difference between m_i and sp_i in this interval for the best fit parameters gives an equivalent width of the methane absorption line.

Evidently it is preferable to observe both Mars and the Moon at the same airmass. However, sometimes it may be difficult to fit this requirement. The suggested correction for airmass by the power function was tested assuming airmasses of Mars of 1.00 and 1.15; that of the Moon was 1.25. For this purpose we calculated
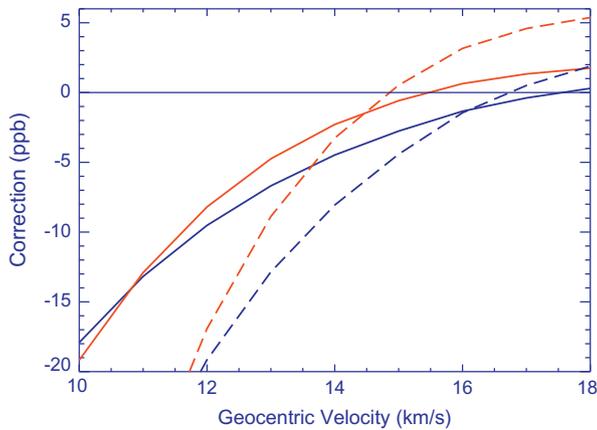
Fig. 5. Correction to methane abundances as functions of geocentric velocity for the blue and red shifts (blue and red, respectively). Solid and dashed lines show calculations for the airmass difference between the Moon and Mars of 0.1 and 0.25 (see Fig. 4). The adopted two-way airmass on Mars is 3. (For interpretation of the references to color in this figure legend, the reader is referred to the web version of this article.)

synthetic spectra of the telluric absorption for the above airmasses and typical conditions of CH_4 (1.75 ppm), H_2O (2 pr. mm), O_3 (0.25 atmo-cm), and p = 0.6 bar above Mauna Kea (Fig. 4). The calculated corrections to extracted methane abundances for various geocentric velocity and two airmass differences of 0.1 and 0.25 are shown in Fig. 5 for a mean airmass of 3 in the martian atmosphere. The calculated corrections are weakly sensitive to the adopted atmospheric abundances. These corrections show that the requirement of the equal airmasses in the observations of Mars and the Moon is not very strict.

5. Observations of methane in December 2009

The Doppler shift was to the blue in the observations on December 7, 2009, and this is not favorable for measurements of methane (Krasnopolsky, 2007; Zahnle et al., 2011). The $^{13}CH_4$ isotopic lines are shifted to the blue by 0.100 cm^{-1} for R0, and two R1 components are shifted by 0.116 and 0.131 cm^{-1}. These values may be compared with the Doppler shift of 0.132 cm^{-1} in the observations on December 7, 2009. The components at the summit of Mauna Kea have transmission ~0.5 and full widths at half maximum of 0.042 cm^{-1}. Therefore the signal at the position of the martian line is smaller for the blue shift than that for the red shift by a factor of ~2 (Fig. 6). In other aspects we do not meet the problem of the contamination by the isotopic lines when comparing the spectra of Mars and the Moon. Airmasses of Mars and the Moon were rather similar, 1.02 and 1.04, during the observations.

One of the observed spectrum of Mars and the properly adjusted spectrum of the Moon are shown in Fig. 6. They are undistinguishable in the figure. Their differences scaled by a factor of 10 and then smoothed within 0.1 cm^{-1} are shown as well. No methane absorption is seen. Standard deviation of the smoothed curve corrected by a factor of $[(33-1)/(33-7)]^{1/2}$ = 1.1 corresponds to the uncertainty of 5 ppb. (33 is the number of pixels for the fitting, and 7 is the number of fitting parameters.)

Spectral exposures were shorter in this observation by a factor of 2 (4 min), the blue shift also reduced the intensity at the martian line position, and the retrieved mixing ratios (Fig. 7) are more uncertain than those in Fig. 2. Mean mixing ratios and their standard deviations are shown in the bottom panel. No methane is seen in the data.

The mean value and standard deviation for the whole R0 panel are 2.4 ppb and 19 ppb. They are shown in the figure. There are
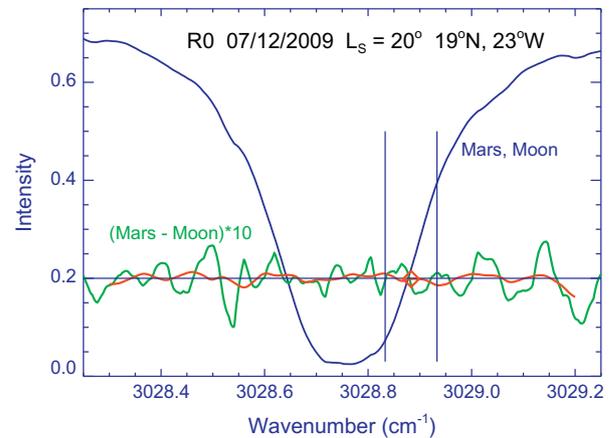

Fig. 6. Spectrum of Mars and the adjusted spectrum of the Moon (blue), their difference scaled by a factor of 10 (green), and that smoothed within 0.1 cm^{-1} (red). The diamond shows the averaged difference at the expected Doppler-shifted position of the martian line. The martian absorption is near zero. The signal at the blue-shifted martian line is weaker than that at the red-shifted line in Fig. 1 by a factor of ~2. (For interpretation of the references to color in this figure legend, the reader is referred to the web version of this article.)
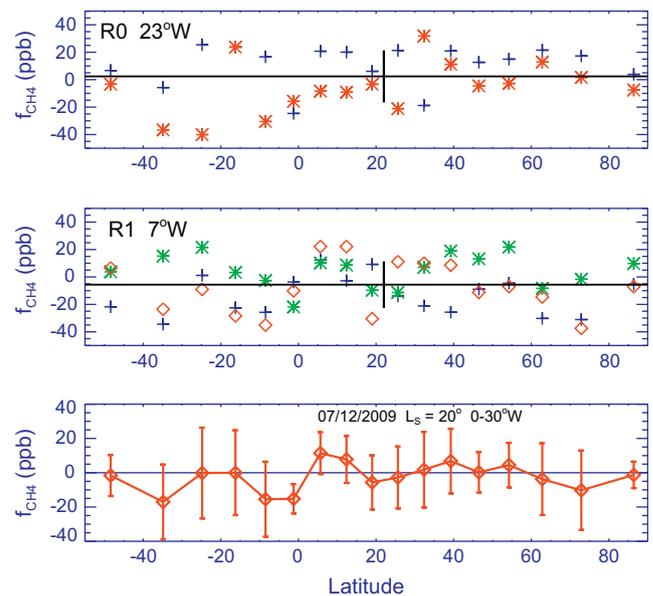

Fig. 7. Results of the observation of methane on Mars in December 2009. Different symbols refer to different spectral frames. Horizontal lines show mean values in the panels, and vertical bars depict standard deviations. Uncertainties of the mean values are quarters of the standard deviations in the upper and middle panels. The lower panel shows mean values and standard deviations for each latitude.

17 points in each panel, and uncertainty of the mean value is a quarter of the standard deviation: 2.4 ± 4.7 ppb. The similar value for the R1 panel is −5.6 ± 4.2 ppb. The uncertainties are weakly overlapping, indicating a possible systematic error. Then the mean of the two mean values is f_{CH4} = −1.6 ± 5.6 ppb. It may be compared with the weighted-mean value for the lower panel, which is f_{CH4} = −2.3 ± 3.4 ppb. Two-sigma upper limits for the mean methane abundance in this observation are 10 and 5 ppb, respectively.

This result obtained at L_S = 20° agrees with our observations and those by Mumma et al. (2009) in February 2006 at the similar season L_S = 10° and 17°, respectively. The PFS zonally-averaged seasonal–latitudinal map (Geminale et al., 2011) gives ~30 ppb at L_S = 20° and 50°S to 70°N. The PFS map for northern spring gives

variations of methane from ~7 to ~70 ppb with a mean value ~40 ppb in the region of our observations. The mean TES data (Fonti and Marzo, 2010) for our region in northern spring ($L_S \approx 0°$) are ~25, 17, and 7 ppb in 2000, 2002, and 2004, respectively.

6. Search for ethane

We searched for ethane on Mars using the IRTF/CSHELL in October 2007. The best way to detect ethane by our instrument is to observe its $^PQ_3$ subband that peaks at 2976.79 cm^{-1}. Villanueva et al. (2012) reanalyzed the C_2H_6 band at 3.3 µm and made some improvements relative to its description in HITRAN-2008. The major improvement for the $^PQ_3$ subband is a contribution from a hot $v_7 + v_4 - v_4$ band with the lower level at 289 cm^{-1}. The hot subband peaks at 2976.86 cm^{-1}, and its strength is ~0.15 and 0.2 of that of $^PQ_3$ at 215 and 250 K, respectively. Their data are not available as software for public use, and we will apply HITRAN-2008 for the $^PQ_3$ subband and add the hot subband.

A sum of the ethane line strengths at 215 K within an interval of 0.1 cm^{-1} centered at this subband is equal to 4.1×10^{-19} cm. The data processing is similar to that for the methane spectra except that we do not care of ethane spatial distribution and summed up all martian spectra. The obtained spectrum is shown in Fig. 8. It consists of telluric lines of methane and water.

A small fragment of this spectrum near the expected positions of the telluric and martian subbands of C_2H_6 is shown in Fig. 9. The spectrum in Fig. 9 is fitted by a synthetic spectrum with the following parameters: continuum, two wavenumber corrections, spectral resolution, telluric and martian ethane abundances. Telluric H_2O and O_3 are fixed at 3.3 pr. mm and 3 mm-atm based on our other observations at that date.

The spectrum includes the Doppler-shifted P7 line of the recently discovered CO^{18}O band at 3.3 µm (Wilquet et al., 2008; Villanueva et al., 2008). The line strength is 8.75×10^{-26} cm at 296 K (Wilquet et al., 2008). It is equal to 1.23×10^{-25} cm at 215 K, calculated using a relationship from Krasnopolsky et al. (2007). Scaled to the ^{18}O/^{16}O isotope ratio, the line strength is 4.9×10^{-28} cm at 215 K.

Fitting by the synthetic spectrum gives a very small negative value for the martian ethane abundance. Therefore the least square fit synthetic spectrum is shown without martian ethane (Fig. 9). The difference between the measured and synthetic spectra and this difference smoothed within 0.1 cm^{-1} are also shown in Fig. 9. The difference spectrum has a wavelike structure with a period of two
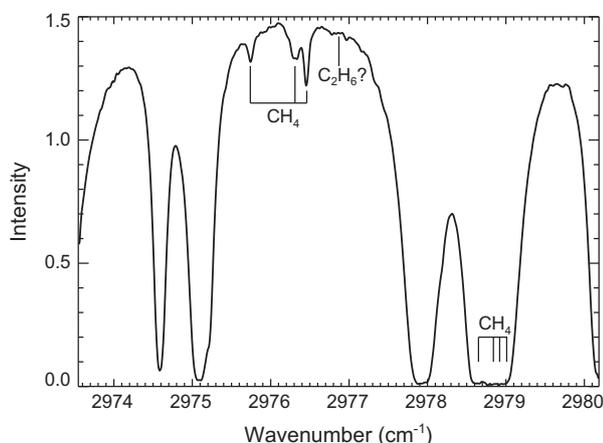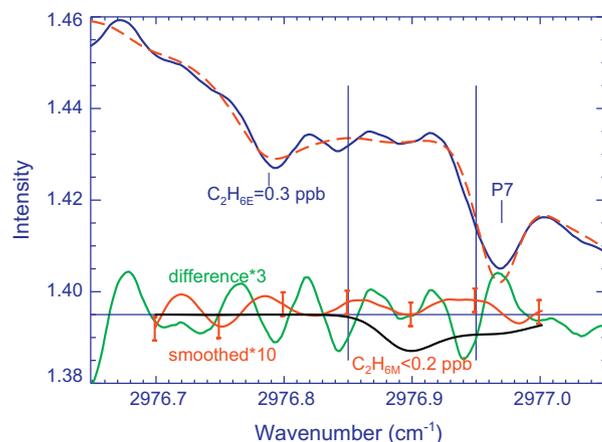

Fig. 9. Fragment of the spectrum in Fig. 8 near the C_2H_6 subband at 2976.79 cm^{-1} (blue solid line) is least-square fitted by a synthetic spectrum (red dashed line). The best fit shown here is without martian ethane. Their difference scaled by a factor of 3 is in the lower part of the figure (green line). This difference smoothed within 0.1 cm^{-1} and scaled by a factor of 10 is shown by the red line. Error bars for this line are corrected for the number of fitting parameters. An interval of 0.1 cm^{-1} centered at the expected Doppler-shifted position of the ethane band is shown by the vertical lines. The black line is a synthetic spectrum of martian ethane with a mixing ratio of 0.2 ppb; its scale is that of the smoothed difference. Retrieved mixing ratio of the Earth's ethane and upper limit to Mars ethane are given, and position of the recently discovered Doppler-shifted P7 line of CO^{18}O is shown. (For interpretation of the references to color in this figure legend, the reader is referred to the web version of this article.)

pixels. This structure reflects imperfect adjustment between the even and odd pixels in the instrument and almost disappears in the smoothed spectrum, because 0.1 cm^{-1} is close to two periods. Standard deviation of this averaged difference is corrected for the significant number of the fitting parameters. Then the retrieved ethane mixing ratio is f_{C2H6} = 0.0 ± 0.08 ppb. An upper limit to ethane on Mars is 0.2 ppb from this observation, and a spectrum for this abundance and the instrument spectral resolution is shown (black line). The previous upper limit was based on the Mariner 9 IRIS spectrum and equaled 400 ppb (Maguire, 1977). Recently this limit was significantly improved to 0.8 ppb (Villanueva et al., 2012). The observed column abundance of ethane in the overhead Earth's atmosphere above Mauna Kea is equal to 2.6×10^{15} cm^{-2} and corresponds to the methane-to-ethane ratio of ~8000. If ethane is mixed in the Earth's atmosphere, then its mixing ratio is 0.21 ppb. If ethane is strongly depleted above ~12 km (see Villanueva et al. (2012) and references therein), then the observed mixing ratio is ~0.3 ppb. Villanueva et al. (2012) observed the telluric ethane at 0.97 ppb in January 2006. According to Rinsland et al. (1991), ethane in January above Hawaii is near its seasonal peak, and our observations in October are close its seasonal minimum when the ethane abundance is smaller by a factor of 2. Our value is even smaller than those from Rinsland et al. (1991) by a factor of ~1.5.

7. Upper limit to SO$_2$

Our search for SO$_2$ on Mars using TEXES resulted in an upper limit of 1 ppb (Krasnopolsky, 2005), with improvement of the previous upper limit (Encrenaz et al., 1991) by a factor of 30. Recently Encrenaz et al. (2011) made a similar search with TEXES and achieved an upper limit of 0.3 ppb. A sum of nine SO$_2$ line strengths that they used for the extraction is smaller than that of sixteen lines in Krasnopolsky (2005) by a factor of 2. Here we come back to Fig. 3 from Krasnopolsky (2005) that shows a sum of spectral intervals centered at the expected positions of sixteen SO$_2$ lines corrected for their continua. The uncertainties in that figure were
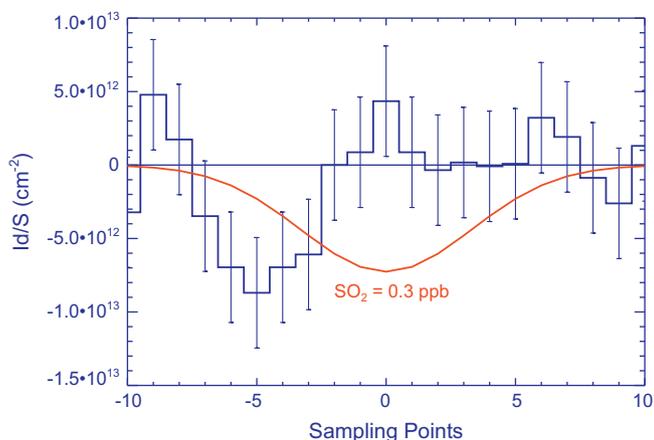

Fig. 8. Spectrum of Mars that was used to search for ethane. Main features are telluric lines of CH$_4$ and H$_2$O.

Fig. 10. Sum of spectral intervals centered at the expected positions of sixteen SO_2 lines and corrected for their continua in the observation by Krasnopolsky (2005). The uncertainties are shown as standard deviation for this curve. Calculated absorption for 0.3 ppb of SO_2 is given for comparison. Its depth is just equal to 2σ.

overestimated and exceed the deviations from zero for all 21 points in the curve that is statistically improbable.

Our Fig. 10 reproduces Fig. 3 from Krasnopolsky (2005) with uncertainties that are equal to the standard deviation of the curve. The curve is compared with a calculated absorption for 0.3 ppb of SO_2. The sampling interval is $d = 0.00228$ cm^{-1}, the resolution element is $8d$, and a sum of the sixteen SO_2 line strengths is $S = 1.0 \times 10^{-18}$ cm. The calculated depth of the SO_2 absorption for its abundance of 0.3 ppb is just equal to 2σ, and our spectrum confirms the upper limit of 0.3 ppb established for SO_2 on Mars by Encrenaz et al. (2011).

The improved upper limit does not change the estimate of 2 years for the SO_2 lifetime (Krasnopolsky, 2005). This lifetime is longer than the estimated time of 0.5 year for global mixing on Mars (Krasnopolsky et al., 2004b) and not favorable to search for local sources of SO_2. The upper limit to global production of SO_2 in Krasnopolsky (2005) should be properly scaled and is equal to 5 ktons per year, smaller than the production on the Earth by a factor of more than 2000.

8. Discussion

Origin of methane on Mars, its variability, and possible heterogeneous loss are discussed in Krasnopolsky (2006), GCM modeling of the methane behavior in the martian atmosphere was made by Lefevre and Forget (2009) and Mischna et al. (2011), and reviews of the problem may be found in Krasnopolsky (2011) and Zahnle et al. (2011).

The refined analysis of our observations in February 2006 at $L_S = 10°$ reveals a region around the deepest canyon Valles Marineris with 10 ppb of methane and ~3 ppb outside this region. The improved technique of search for methane by comparison with the simultaneously measured spectra of the Moon resulted in an upper limit of 8 ppb for the observations in December 2009 at $L_S = 20°$.

The extracted methane abundances are in reasonable agreement with ~3 ppb observed by Mumma et al. (2009) in February 2006 at $L_S = 17°$. The mean TES data (Fonti and Marzo, 2010) for the regions of our observations in the northern spring are ~25, 18, and 10 ppb in 2000, 2002, and 2004, respectively. Although extrapolation of this trend may agree with our results, the latitudinal behavior of methane in the TES maps is opposite to those in our observations and in Mumma et al. (2009). The PFS maps (Geminale et al., 2011) give ~30 ppb for the conditions of our observations. These maps were made assuming no interannual variations of methane.

The mean CH_4 abundances are 10 ppb in the observations by Krasnopolsky et al. (2004a,b) in 1999 and 20 ppb in the observations by Mumma et al. (2009) in 2003. Zahnle et al. (2011) pointed out that those observations in 2003 were Doppler-shifted to the blue and contaminated by the $^{13}CH_4$ lines. However, they mentioned that ^{13}C is depleted in telluric methane relative to the PDB standard adopted in the HITRAN database. Therefore the CH_4 abundances in the observations by Mumma et al. (2009) in 2003 may be underestimated.

Krasnopolsky (2006) argued that the spatial variability of the martian methane requires its heterogeneous loss with a lifetime of $\leqslant 0.5$ y. That estimate was confirmed by GCM simulations by Lefevre and Forget (2009) who found the lifetime of $\leqslant 200$ days. Mumma et al. (2009) estimated the methane lifetime at 4 y or 0.6 y, assuming that the observed abundances at $L_S = 155°$ as either episodic or regular.
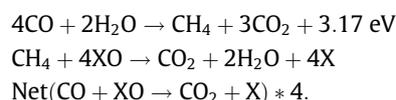
The PFS observations for six years since January 2004 favor stable methane with a global-mean mixing ratio of 15 ppb. The methane abundance varies significantly with season and from place to place (Geminale et al., 2011). A possible source of methane is the north polar and subpolar regions at the end of northern summer. Some features in the PFS methane maps look unexpected. For example, some regions with very high methane ~70 ppb are between regions with no methane. Although the maps were made with a grid of $20° \times 20°$, this contrast is too high to overcome mixing by the atmospheric dynamics. The CH_4 abundances in our observations are smaller than the PFS data.

According to the TES maps of methane (Fonti and Marzo, 2010), the global methane varies significantly with season (declining by a factor of 5 from $L_S = 180°$ to $270°$). Interannual variations are different at different seasons. For example, the global methane decreased at $L_S = 0°$ from 2000 to 2004 by a factor of 2 and increased at $L_S = 90°$ in this period by the same factor. Annually and globally mean methane abundances are similar in MY24/25 (1999–2001) and MY26/27 (2003–2005), 17.5 ppb and 18.0 ppb, respectively, and favor highly variable but generally stable methane.
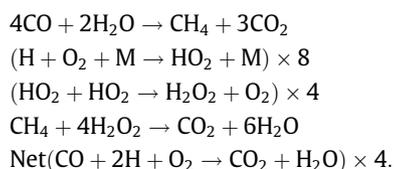
The PFS and TES methane data were collected for 6 years of regular observations from the orbiters and do not need corrections for the absorption by the Earth's atmosphere. However, both resolution and signal-to-noise ratio of both instruments are rather low for observations of methane on Mars. The studies for methane are made by summing a few thousands spectra per each measurement, and some instrumental effects and systematic errors, which are weak in the individual spectra, are not removed by the summing and may become significant.

Krasnopolsky (2006) concluded that the heterogeneous losses of methane in reactions with metal oxides, superoxide ions, and in the classic Fischer–Tropsch process are very slow at the martian conditions to explain the variations of methane. Krasnopolsky (2011) discussed weaknesses of a hypothesis of the intense peroxide production and removal of methane in the dust devils. According to Zahnle et al. (2011), clathrates and adsorption by the surface rocks cannot induce the observed variations of methane as well.

Zahnle et al. (2011) argued that the variable methane is incompatible with the current redox state of the martian atmosphere. However, their argument does not work if methane is made from the atmospheric constituents. The CH_4 production and loss rates are equal to 1.5×10^8 cm^{-2} s^{-1} for $CH_4 = 10$ ppb and the lifetime of 0.5 y. If methane is formed by methanogenic bacteria that eat CO and H_2O and lost in a reaction with XO, then
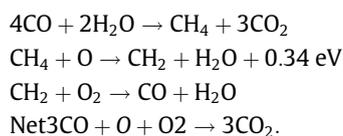
$$4CO + 2H_2O \rightarrow CH_4 + 3CO_2 + 3.17 \text{ eV}$$
$$CH_4 + 4XO \rightarrow CO_2 + 2H_2O + 4X$$
$$\text{Net}(CO + XO \rightarrow CO_2 + X) * 4.$$

The redox state of the atmosphere does not change, and the methane cycle is a minor pathway of the CO_2 association with a rate of 6×10^8 cm^{-2} s^{-1}, which is smaller than the total CO_2 association rate of 7.6×10^{11} cm^{-2} s^{-1} by three orders of magnitude. The loss reaction proceeds at the surface rocks or dust, and X may be nothing, O_2 or H_2O. The case of O_2 is not a problem because the O_3 formation rate is $\sim 3 \times 10^{12}$ cm^{-2} s^{-1}. The case of H_2O is more complicated:

$$4CO + 2H_2O \rightarrow CH_4 + 3CO_2$$
$$(H + O_2 + M \rightarrow HO_2 + M) \times 8$$
$$(HO_2 + HO_2 \rightarrow H_2O_2 + O_2) \times 4$$
$$CH_4 + 4H_2O_2 \rightarrow CO_2 + 6H_2O$$
$$Net(CO + 2H + O_2 \rightarrow CO_2 + H_2O) \times 4.$$

The required loss rates of peroxide and odd hydrogen of 6×10^8 and 1.2×10^9 cm^{-2} s^{-1} may be compared with their production rates of 2.5×10^{10} and 1.9×10^{10} cm^{-2} s^{-1}, respectively. (The above photochemical rates are from Krasnopolsky (2010a).) In this case the odd hydrogen loss in the methane cycle is 6% of its total production. The inclusion of the methane cycle at this rate does not significantly change the current values of hydrogen escape and the surface oxidation.

The simplest version of the methane cycle would be

$$4CO + 2H_2O \rightarrow CH_4 + 3CO_2$$
$$CH_4 + O \rightarrow CH_2 + H_2O + 0.34 \text{ eV}$$
$$CH_2 + O_2 \rightarrow CO + H_2O$$
$$Net 3CO + O + O2 \rightarrow 3CO_2.$$

Actually the observed products in the second reaction are $CH_3 + OH$ and $CH_3O + H$, and these branches are endothermic and very slow at the martian temperatures. Therefore, the suggested branch requires a heterogeneous catalysis. This cycle does not involve odd hydrogen.

Our search for ethane on Mars results in an upper limit of 0.2 ppb. According to Allen et al. (2006), the CH_4/C_2H_6 ratio strongly depends on the origin of hydrocarbons and is typically smaller than 300 for geological sources and exceeds 300 for biological sources. Measurements of this ratio are a way to establish the origin of methane on Mars.

Photochemical loss of ethane on Mars is faster than that of methane by a factor of 25 (Krasnopolsky, 2006) because of the much faster reaction with OH. However, almost nothing is known on heterogeneous chemistry of methane and ethane on Mars. Ethane in the martian atmosphere may be strongly depleted relative to the source value, and prospects of ethane detection are poor. No conclusion on the origin of methane on Mars can be drawn from the observed upper limit.

The very low upper limit to SO_2 on Mars does not favor geological methane that is less abundant than SO_2 in the outgassing from the terrestrial planets. The lack of hot spots with endogenic heat sources in the THEMIS observations does not support the geological methane as well.

9. Conclusions

The IRTF/CSHELL observations in February 2006 at $L_S = 10°$ and 63–93°W show ~ 10 ppb of methane at 45°S to 7°N and ~ 3 ppb outside this region. This region covers the deepest canyon Valles Marineris.

Observations in December 2009 at $L_S = 20°$ and 0–30°W included measurements of the Moon spectrum at a similar airmass as a telluric calibrator. A technique for extraction of the martian methane line from a combinations of the Mars and Moon spectra

has been developed. The observations were at the Doppler shift to the blue and reveal no methane with an upper limit of 8 ppb.

The results of both sessions agree with the observations by Mumma et al. (2009) at the same season in February 2006. The retrieved methane abundances are smaller than those in the PFS (Geminale et al., 2011) and TES (Fonti and Marzo, 2010) maps.

If methane is biological on Mars, its production and removal do not significantly change the redox state of the atmosphere and the balance of hydrogen.

Our search for ethane at 2977 cm^{-1} results in an upper limit of 0.2 ppb. However, this limit does not help to establish the origin of methane on Mars.

Revision of the TEXES observations of SO_2 (Krasnopolsky, 2005) results in an improvement of the upper limit to SO_2 on Mars to the value of 0.3 ppb. This limit confirms the recent result by Encrenaz et al. (2011).

Along with the lack of hot spots with endogenic heat sources in the THEMIS observations, the very low upper limit to SO_2 on Mars does not favor geological methane that is less abundant than SO_2 in the outgassing from the terrestrial planets.

References

Allen, M., Lollar, B.S., Runnegar, B., Oehler, D.Z., Lyons, J.R., Manning, C.E., Summers, M.E., 2006. Is Mars alive? EOS Transactions. AGU 87, 433–439.
Conrath, B.J. et al., 2000. Mars Global Surveyor Thermal Emission Spectrometer (TES) observations: Atmospheric temperatures during aerobraking and science phasing. J. Geophys. Res. 105, 9509–9520.
Encrenaz, T. et al., 1991. The atmospheric composition of Mars: ISM and ground-based observational data. Ann. Geophys. 9, 797–803.
Encrenaz, T. et al., 2011. A stringent upper limit to SO_2 in the martian atmosphere. Astron. Astrophys. 530, A37.
Fonti, S., Marzo, G.A., 2010. Mapping the methane on Mars. Astron. Astrophys. 512, A51. doi:10.1051/0004-6361/200913178/3.141592654.
Formisano, V., Atreya, S., Encrenaz, T., Ignatiev, N., Giuranna, M., 2004. Detection of methane in the atmosphere of Mars. Science 306, 1758–1761.
Geminale, A., Formisano, V., Sindoni, G., 2011. Mapping methane in Martian atmosphere with PFS-MEX data. Planet. Space Sci. 59. doi:10.1016/j.pss.201007.011.
Hase, F., Wallace, L., McLeod, S.D., Harrison, J.J., Bernath, P.F., 2010. The ACE-FTS atlas of the infrared solar spectrum. J. Quant. Spec. Rad. Trans. 111, 521–528.
Krasnopolsky, V.A., 2005. A sensitive search for SO_2 in the Martian atmosphere: Implications for seepage and origin of methane. Icarus 178, 487–492.
Krasnopolsky, V.A., 2006. Some problems related to the origin of methane on Mars. Icarus 180, 359–367.
Krasnopolsky, V.A., 2007. Long-term spectroscopic observations of Mars using IRTF/CSHELL: Mapping of O_2 dayglow, CO, and search for CH_4. Icarus 190, 93–102.
Krasnopolsky, V.A., 2010a. Solar activity variations of thermospheric temperatures on Mars and a problem of CO in the lower atmosphere. Icarus 207, 638–647.
Krasnopolsky, V.A., 2010b. Spatially-resolved high-resolution spectroscopy of Venus. 2. Variations of HDO, OCS, and SO_2 at the cloud tops. Icarus 209, 314–322.
Krasnopolsky, V.A., 2011. Atmospheric chemistry on Venus, Earth, and Mars: Main features and comparison. Planet. Space Sci. 59, 952–964.
Krasnopolsky, V.A., Bjoraker, G.L., Mumma, M.J., Jennings, D.E., 1997. High-resolution spectroscopy of Mars at 3.7 and 8 µm: a sensitive search for H_2O_2, H_2CO, HCl, and CH_4, and detection of HDO. J. Geophys. Res. 102, 6525–6534.
Krasnopolsky, V.A., Maillard, J.P., Owen, T.C., 2004a. Detection of methane in the martian atmosphere: Evidence for life. In: EGU Congress, April 2004, Geophys. Res. 6. Abstract 06169.
Krasnopolsky, V.A., Maillard, J.P., Owen, T.C., 2004b. Detection of methane in the martian atmosphere: Evidence for life? Icarus 172, 537–547.
Krasnopolsky, V.A., Maillard, J.P., Owen, T.C., Toth, R.A., Smith, M.D., 2007. Oxygen and carbon isotope ratios in the martian atmosphere. Icarus 192, 396–403.
Lefevre, F., Forget, F., 2009. Observed variations of methane on Mars unexplained by known atmospheric chemistry and physics. Nature 460, 720–723.
Maguire, W.C., 1977. Martian isotopic ratios and upper limits for possible minor constituents as derived from Mariner 9 infrared spectrometer data. Icarus 32, 85–97.

Mischna, M.A., Allen, M., Richardson, M.I., Newman, C.E., Toigo, A.D., 2011. Atmospheric modeling of Mars methane surface release. Planet. Space Sci. 59. doi:10.1016/j.pss.201007.005.

Mumma, M.J. et al., 2009. Strong release of methane on Mars in northern summer 2003. Science 323, 1041–1045.

Rinsland, C.P., Goldman, A., Murcray, F.J., David, S.J., Blatherwick, R.D., Murcray, D.G., 1991. Infrared spectroscopic measurements of the ethane (C_2H_6) total column abundance above Mauna Loa, Hawaii – Seasonal variations. J. Quan. Spect. Rad. Transfer 52, 273–279.

Smith, M.D., 2004. Interannual variability in TES atmospheric observations of Mars during 1999–2003. Icarus 167, 148–165.

Villanueva, G.L., Mumma, M.J., Novak, R.E., Hewagama, T., 2008. Discovery of multiple bands of isotopic CO_2 in the prime spectral regions used when searching for CH_4 and HDO on Mars. J. Quant. Spect. Rad. Trans. 109, 883–894.

Villanueva, G.L., Mumma, M.J., Magee-Sauer, K., 2012. Ethane in planetary and cometary atmospheres: Transmittance and fluorescence models of the v_7 band at 3.3 μm. J. Geophys. Res. doi:10.1029/2011JE003950.

Wilquet, V. et al., 2008. Line parameters for the 01111–00001 band of $^{12}C^{16}O^{18}O$ from SOIR measurements of the Venus atmosphere. J. Quant. Spec. Rad. Trans. 109, 895–905.

Zahnle, K., Freedman, R.S., Catling, D.C., 2011. Is there methane on Mars? Icarus. doi:10.1016/j.icarus.2010.11.027.